CrossMark

RESEARCH PAPER

Development and testing of a high-chromium, Ni-based filler metal resistant to ductility dip cracking and solidification cracking

Adam T. Hope[1] · John C. Lippold[1]

Abstract Ni-based filler metals for repair and construction of nuclear reactor components require 30 wt% Cr to insure resistance to primary water stress corrosion cracking (PWSCC). Current generation alloys can be susceptible to solidification cracking and ductility dip cracking, depending on Nb content and the amount of eutectic that forms during weld solidification. Computational thermodynamic modeling was used to identify alternative eutectic-forming elements to Nb, such as Hf and Ta. Previous work has utilized a design of experiment methodology (DOE) in conjunction with computational and experimental techniques to optimize a new filler metal composition that should be resistant to weld cracking. In this paper, the optimized compositions were subjected to further weldability testing, namely the cast pin tear test (CPTT) and the strain-to-fracture (STF) test. An optimized Ta-bearing composition was found to be crack resistant, while an optimized Hf-bearing composition was highly susceptible to solidification cracking. Differences may be related to the nature of the eutectic constituents that form at the end of solidification. The Hf-bearing composition did not form Laves phase as its final eutectic constituent, while Laves is present in both the Nb- and Ta-bearing systems.

Recommended for publication by Commission IX - Behaviour of Metals Subjected to Welding

✉ Adam T. Hope
hope.30@buckeyemail.osu.edu

[1] Welding Engineering Program, Department of Materials Science and Engineering, The Ohio State University, Columbus, OH, USA

1 Background

The nuclear power industry uses nickel-based filler metals containing significant levels of Cr (20–30 wt%) to join dissimilar metals. Alloys with less than 25 wt% Cr, such as FM82 (ERNiCr-3), have been found to be susceptible to primary water stress corrosion cracking (PWSCC). Because of this, alloys such as FM52 and FM52M (ERNiCrFe-7/7A), with approximately 30 wt% Cr, are currently used for repair welding and overlays of nuclear pressure vessel components in pressurized water reactors (PWR) and are proposed for use in new construction [1–5].

While resistant to PWSCC, FM52 was found to be susceptible to ductility dip cracking (DDC) [6]. This type of cracking is associated with the migration of solidification grain boundaries and subsequent stress build up along these boundaries. Migrated boundaries in susceptible alloys become very straight, and due to excessive sliding at intermediate temperatures, cracks can form. To prevent this form of cracking, the addition a few wt% Nb causes a eutectic to form at the end of solidification, which pins the solidification grain boundaries, preventing them from becoming straight and reducing crack susceptibility [6]. Alloys have been developed with a few wt% Nb, such as FM52i and FM52MSS (ERNiCrFe-13) that have an increased resistance to DDC.

However, increasing the Nb content in these alloys causes an increased susceptibility to solidification cracking [7, 8]. This is related to Nb-rich eutectic constituents that form at the end of solidification and expand the solidification temperature range (STR). DuPont et al. [9] found a correlation between solidification temperature range and solidification cracking susceptibility for Nb-bearing compositions. Alloys with lower Nb, such as FM52M, have greater resistance to solidification cracking [7, 10].

Due to the competing effects of Nb in high-Cr Ni-based alloys (DDC vs. solidification cracking), a fine balance is

Springer

needed with respect to composition to avoid both forms of cracking. This work investigates replacing Nb with either Ta or Hf to promote the formation of eutectic phases at the end of solidification, but with a higher terminal eutectic temperature than that of current alloy compositions. This will allow eutectic constituents to be generated during weld metal solidification for DDC resistance while keeping the solidification temperature range narrow for solidification cracking resistance.

Baeslack et al. [11] investigated substituting Ta for Nb in Alloy 718 weld metal and performed varestraint weldability testing. Gleeble® heat-affected zone tests were also performed to determine the liquation temperature. The authors found improvement in liquation and solidification cracking for the alloys with Ta substituted for Nb. They attributed this to the higher liquation temperature of the Ta-rich γ/Laves eutectic relative to the Nb-rich γ/Laves eutectic. The liquation temperatures of the Laves phases were 1225 and 1175 °C, respectively.

Hafnium is another potential replacement for Nb in these high Cr nickel base alloys. Historically, Hf has been added to cast superalloys to modify the grain boundary carbide morphology [12]. MC carbides form upon solidification and are generally Hf-rich [13]. A study by Dmitrieva et al. [14] found the γ/HfC eutectic to solidify at 1330 °C. Furthermore, a study by Nash and West [15] found no evidence of Laves phase in a ternary Ni-Cr-Hf system. Nash and West [15] melted samples of varying composition and determined the solidus temperature, as well as phases present by XRD. They found that γ/Ni_7Hf_2 eutectic formed when 30 at% Cr was present at a temperature of 1288 °C. This is promising because when carbon is exhausted on solidification, other eutectic phases such as Laves may form in systems containing Nb or Ta. The Ni_7Hf_2 phase, which could form when Hf is present and C has been exhausted, has a much higher eutectic temperature than both the Nb or Ta-rich Laves eutectics. This is expected to improve solidification cracking resistance over Nb or Ta eutectics by narrowing the solidification temperature range.

2 Experimental

2.1 Development of optimized filler metal composition

The first part of this investigation attempted to identify compositions that use alternative eutectic forming elements to Nb. Much of early work can be found elsewhere [16]. Based on the literature review and extensive thermodynamic calculations using Thermo-Calc®, Ta, Hf, and Mo were selected as potential replacements for Nb. Varying amounts of these elements were added to a base composition of Ni-30Cr (wt%). The Fe content was also varied slightly to determine how dilution with steels might play a role on eutectic formation. A set of compositions containing Nb was also tested as a baseline.

A design of experiment methodology (DOE) was used to generate a set of alloy compositions that would allow determination of the elemental effects on solidification temperature range (STR) and the fraction eutectic. These responses were selected to represent cracking susceptibility, since STR has been shown to have a strong effect on solidification cracking susceptibility [9], and a sufficient level of eutectic formed at the end of solidification can prevent DDC. A thermo-couple plunging technique along with single sensor differential thermal analysis (SSDTA) was used to determine the STR. Metallographic image analysis was used to determine the fraction eutectic.

Initially, a range of compositions was chosen and simulated using the Scheil module within Thermo-Calc® and entered into the DOE model. Based on these results, compositions were selected for experimental weldability testing also using the DOE. Finally, an optimized composition was generated using the data. To optimize a composition, a target of 2 vol% eutectic and a STR of less than 150 °C were selected. Metallographic image analysis of weld metals known to be resistant to DDC has shown that they generally have greater than 2 vol% eutectic [17]. DuPont et al. [9] have shown that alloys with a STR less than 150 °C are resistant to solidification cracking. More details on the steps taken to optimize the filler metal composition has been published in [16]. This paper will focus on the subsequent weldability testing that was performed on the optimized alloy compositions.

2.2 Weldability testing of optimized compositions

To evaluate the weldability of select compositions of material, weldability tests that can accommodate limited quantities of material were chosen. To evaluate solidification cracking susceptibility, the cast pin tear test (CPTT) was used. To evaluate DDC susceptibility, a slightly modified Strain to Fracture (STF) test was used. It would have been desirable to also perform transvarestraint testing, or an unmodified STF test; however, these tests require a significant amount of filler metal wire to create V-groove welds that are used for sample coupons.

2.2.1 Cast pin tear testing

A new design of the CPTT, modified by Luskin and Alexandrov [18, 19], was used to evaluate solidification crack susceptibility. This new design uses an induction coil to melt and feed pin-shaped copper molds of varying length with the material of interest. Solidification stresses build up in the molds as a function of the mold length, and if the stresses are high enough (as pin length increases), solidification cracks form. Materials that are susceptible to solidification cracking will crack at shorter mold lengths than more resistant alloys. This way the solidification cracking susceptibility of different alloys can be compared. Figure 1 (left) shows a schematic of
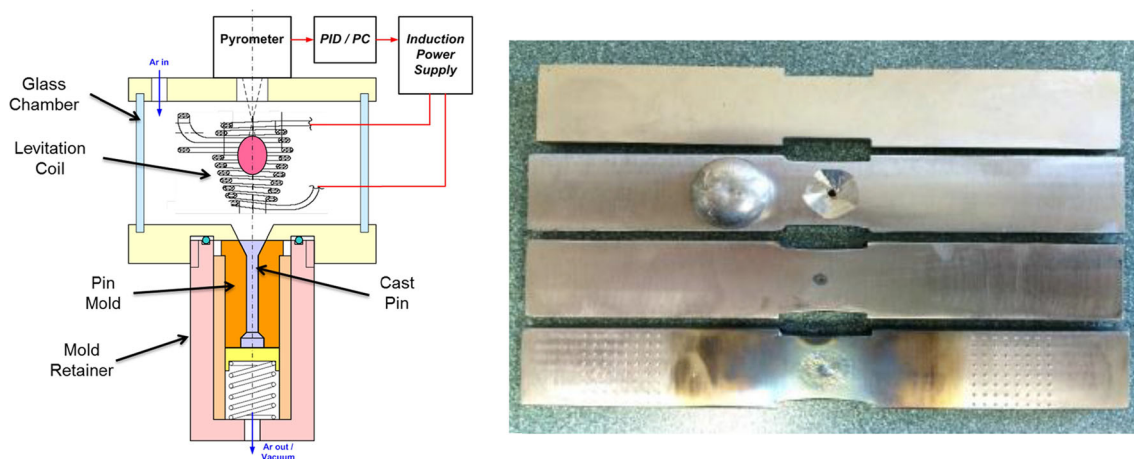
Fig. 1 Schematic of the updated cast pin tear testing (CPTT) device developed at OSU [19] (*left*); and typical strain-to-fracture (STF) sample at various sample preparation steps using the limited material procedure (*right*)

the setup. Three or more pins are cast at each mold length and the pin with the most cracking is recorded. Reporting of maximum cracking instead of average cracking has been shown to correlate better with industry experience of crack susceptibility [10]. Additionally, Przybylowicz [10] defined the threshold for cracking, the longest pin length where no cracking is observed, for comparing alloy susceptibility. This is referred to as the Lower Cracking Threshold (LCT).

2.2.2 Strain-to-fracture test

The STF test was developed by Nissley and Lippold [17] to simulate and rank DDC susceptibility in nickel-base alloys and austenitic stainless steels. The test uses a dogbone tensile sample that is either machined out of an all-weld metal coupon, or is machined from a V-groove coupon such that the reduced gauge section is comprised entirely of weld metal. A GTA spot weld is made on the gauge section with carefully controlled parameters specified in [17]. The purpose of this spot weld is to develop a uniform microstructure in the sample (eliminating local variations that may occur in multipass welds), as well as create grain boundaries that are oriented at all angles with respect to the loading direction. The sample is then placed in the Gleeble, where it is heated to 950 °C, held for 10 s, and pulled to a pre-determined strain level at a stroke rate of 0.06 cm/s. The sample is then allowed to free cool and is inspected for DDC cracks. The spot welding and Gleeble® test parameters have recently been investigated for robustness. Kreuter [20] used a DOE matrix of parameters and found that the parameters originally recommended by Nissley and Lippold [17] produced clear differences in alloy susceptibility and were tolerant to slight variations.

Due to limitations on material, dogbone STF samples could not be machined from full-size weld coupons. To overcome this limitation, a novel sample design was used, which has been previously demonstrated to be effective by Sowards

[21]. Samples of alloy 690 were machined to the standard STF dogbone geometry. A conical hole was drilled into the face of the gauge section, where 5-g buttons of desired composition were placed. The button was manually melted into the sample using a GTAW torch. The surface was ground flat, and the standard STF spot weld procedure was then carried out (140A, 11 V for 10 s, 12.7 s current downslope). Dilution was calculated to be less than 20% by examining weld cross sections of pre-ground samples. Figure 1 (right) shows a typical STF sample and the steps used to create it.

2.3 Metallurgical characterization

To prepare samples for light optical and scanning electron microscopy, weldability test samples were cross sectioned and mounted in conductive Bakelite. Samples were ground with SiC papers from 240 to 800 grit and polished with diamond compound from 9 to 1 μm. A final vibratory polish was performed using 0.05 μm colloidal silica on a Buehler Vibromet for 2–4 h. A 10% chromic acid electrolytic etch was used at 5 V for 2–10 s. Scanning electron micrographs were taken using a Philips LX-30 ESEM operating at 10–20 keV. In some cases, energy dispersive spectroscopy (EDS) was performed to obtain compositional information. X-rays were collected with an EDAX brand silicon drift detector.

3 Results and discussion

3.1 Computational modeling

Prior to the design of experiment and optimization work, Thermo-Calc® was used to generate pseudo-binary phase diagrams to determine terminal eutectic temperatures. This approach can provide a general idea of the maximum STR in a given alloy system, given that the liquidus values do not

change much over the composition space. Higher terminal eutectic temperatures indicate a narrower STR and a reduced solidification cracking susceptibility. The TCNI5 database was used for all calculations. The carbide former (Nb, Ta, or Hf) was varied along with carbon, while Cr and Fe were fixed at 30 and 8 wt%, respectively.

Table 1 summarizes the results of the calculated pseudo-binary phase diagrams. In a Ni-30Cr system containing carbon, a γ-MC eutectic is predicted to form with Nb, Ta, and Hf. For Ta and Hf, the γ-MC eutectic forms at a higher temperature than the Nb γ-MC eutectic. When carbon is exhausted, a γ-Laves eutectic forms when Nb or Ta is present. This severely lowers the terminal eutectic temperature, which could increase solidification cracking susceptibility, although there is a slight advantage in using Ta over Nb due to the slightly higher terminal solidification temperature, 1190 and 1160 °C, respectively. When Hf is present, a γ-Laves eutectic is not predicted to form, and instead a γ-Ni₇Hf₂ eutectic forms at 1250 °C. This reaction would keep the STR narrow even if carbon is exhausted during solidification due to the formation of a γ-MC eutectic. A recent study by Feng et al. [22] verified the eutectic temperature and crystal structure of γ-Ni_7Hf_2 in a Hf-bearing Ni-30Cr alloy via selected area diffraction in the TEM.

3.2 Optimized compositions from DOE

More details on the DOE and the experimental optimization can be found in [16]. The major results from this work were two sets of optimized alloy compositions, one Hf-bearing and one Ta-bearing, as shown in Table 2. An effect of Mo could not be determined, so compositions with and without Mo were selected for further weldability testing. The optimized level of Hf was found to be 0.75 wt% using the experimental DOE; however, preliminary testing showed that the solidification cracking resistance at this level was poor, as no pins could be cast without cracks. For this reason, Hf was reduced to 0.25 wt% to further reduce the STR. The STR was reduced from 150 to 115 °C, as determined by thermo-couple plunges and SSDTA. This unexpected cracking behavior of the optimized Hf composition may be related to the nature of the eutectic that forms and is discussed is the following section.

The nominal compositions in Table 2 were used to create commercially cast and drawn filler wires for further testing. Compositions of the actual wires are shown in Table 3. These

Table 1 Summary of terminal eutectic temperatures determined from calculated pseudo-binary phase diagrams

	γ-MC eutectic (°C)	γ-Laves eutectic (°C)	γ-Ni₇Hf₂ eutectic (°C)
Nb	1280	1160	
Ta	1330	1190	
Hf	1310		1250

Table 2 Nominal compositions (wt%) of optimized compositions

Alloy	Ni	Fe	Fe	Mo	C	Hf or Ta
52-Hf	Bal.	30	8	0	0.04	0.25
52-Hf-Mo	Bal.	30	8	4	0.04	0.25
52-Ta	Bal.	30	8	0	0.04	4
52-Ta-Mo	Bal.	30	8	4	0.04	4

filler metals were then subjected to the CPTT and STF tests as described previously.

3.3 CPTT testing

Since the CPTT test can only rank alloy susceptibility to solidification cracking, a baseline for susceptible and resistant alloys was needed. Przybylowicz [10] used the third-generation CPTT with the optimized parameters that Luskin and Alexandrov [18, 19] developed to test a wide range of alloys and to compare them with industry experience. FM52MSS-C, a current generation high-Cr alloy with 3.5 wt% Mo and 2.5 wt% Nb, is known to be moderately susceptible to solidification cracking. FM82, with 0 wt% Mo and 2.4 wt% Nb, is considered resistant to solidification cracking under moderate restraint conditions based on industry experience. The compositions of these materials can be seen in Table 4. Both of these alloys are also quite resistant to DDC because of the amount of eutectic they form based on their similar Nb contents. Also, the resistance of FM82 to solidification cracking is associated with its lower Cr and Fe contents. In FM52MSS-C, the additional Cr and Fe promote the formation of γ/Laves eutectic, which widens the STR.

The alloy compositions in Table 3 were tested using the third-generation CPTT with the parameters optimized by Luskin and Alexandrov [18, 19] to be comparable to the data from Przybylowicz [10, 18]. Due to limitations in the amount of material, not all mold lengths could be tested, so most material was used to determine the LCT instead of testing the full range of pin lengths. The results are shown in Fig. 2. The Ta-bearing alloys no. 3 and no. 4 performed as expected, with and LCT of 1.0-in. pin length. This predicts cracking resistance better than 52MSS-C (LCT = 0.75) and slightly worse than FM82 (LCT = 1.25). There appears to be no significant effect of Mo on the solidification cracking resistance in the Ta-bearing alloys.

The CPTT results for the Hf-bearing alloys no. 1 and no. 2 were unexpected. The LCT was at the shortest pin length possible to cast (0.625 in.), predicting solidification cracking resistance worse than 52MSS-C. These results were unexpected since the STR for alloy no. 1 was experimentally determined to be 115 °C. This contradicts the widely held belief that the width of the STR correlates with solidification crack susceptibility. This contradictory behavior is thought to be related to a wetting effect of the eutectic liquid and the ability

Table 3 Compositions (wt%) of commercially cast and drawn wires used for weldability testing

	Ni	Cr	Fe	Mo	Hf	Ta	C	Al	Ti
Alloy #1-Hf	Bal.	28.43	12.3	<0.005	0.24	<0.005	0.043	0.017	<0.002
Alloy #2-Hf-Mo	Bal.	29.67	8.41	3.87	0.25	<0.002	0.036	0.025	0.002
Alloy #3-Ta	Bal.	29.83	7.99	<0.005	<0.01	3.88	0.035	0.007	0.004
Alloy #4-Ta-Mo	Bal.	29.76	8.05	3.86	<0.01	3.82	0.033	0.010	0.003

Table 4 Commercial alloys that are known to be susceptible (52MSS-C) and resistant (FM82) to solidification cracking that were used as baselines for comparison in the CPTT

	Ni	Cr	Fe	Mo	Nb	C	Al	Ti
FM52MSS-C	Bal	29.24	8.79	3.51	2.51	0.02	0.13	0.18
FM82 (YB8908)	Bal	19.15	0.98	–	2.38	0.044	0.021	0.37

to form continuous liquid films along the grain boundary. This is the subject of an ongoing investigation. Again, there was no discernible effect of Mo on the solidification cracking resistance in the Hf-bearing alloys.

3.4 STF testing

Limited modified STF testing was conducted by preparing small buttons of the Hf-bearing alloy composition Ni-30Cr-8Fe-0.25Hf-0.04C and the Ta-bearing composition Ni-30Cr-8Fe-4Ta-0.04C (in wt%). Because of material limitations, only a few tests were performed for each composition to determine the threshold strain to fracture.

The results from the STF tests are shown in Fig. 3. Data from two other alloys, tested previously by Lippold and Nissley [6], FM52M and FM52MSS, are plotted for reference. This is to show how a DDC-susceptible (FM52M) and a resistant (FM52MSS) alloy perform in the STF test. The most important metric for ranking the DDC susceptibility is the threshold strain to fracture at a test temperature of 950 °C. The threshold strain is defined as the highest strain that can be applied in the STF test without the occurrence of cracking. The Ta-bearing composition, which has the same amount of

Ta (at%) as Nb (at%) in FM52MSS, has a very similar response to FM52MSS (threshold strain 10% vs. 9% respectively). The Hf-bearing composition has a slightly higher DDC susceptibility, based on a threshold strain of ~5%). However, its threshold is still significantly higher than that of FM52M and would likely be more resistant than FM52M in actual practice.

3.5 Metallurgical characterization

Metallographic cross sections of select cast pins were used to assess the nature of the eutectic constituent that forms during solidification in the different alloy compositions. Figure 4 shows SEM micrographs of the Ta-bearing alloys no. 3 and no. 4. The general nature and distribution of the eutectic is very similar with and without 4 wt% Mo additions. The eutectic is evenly distributed along subgrain boundaries and exists as discreet particles. No evidence of eutectic "spreading" along subgrain boundaries was found. Qualitative EDS showed enrichment of Ta and C in the eutectic particles when compared to the matrix for both alloys. In alloy no. 4, the interdendritic regions were enriched in Mo. The eutectic constituents were too small (<2 μm) to determine whether Mo was present within the eutectic or just enriched in the area around the eutectic. It was not feasible to assess migrated grain boundary character in the cast pin samples, as the cooling rate is quite fast after solidification, which limits time for grain boundary migration.

Figure 5 shows SEM micrographs of the Hf-bearing cast pins. Some small discrete eutectics were found in the interdendritic regions, and occasionally long "spread out" eutectics could be found along subgrain boundaries. It is not
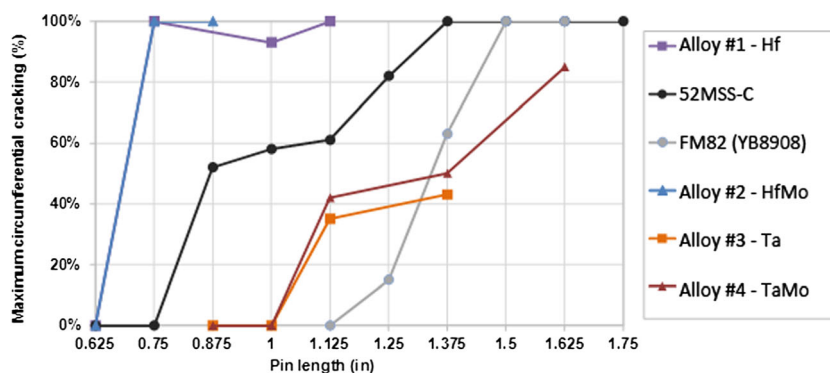
Fig. 2 CPTT results of optimized compositions in Table 3. 52MSS-C and FM82 data [10] is added for comparison

Fig. 3 STF results of optimized Hf- and Ta-bearing compositions, without Mo. Data of FM52M, which is known to be susceptible to DDC, and FM52MSS, which is DDC resistant, are shown for comparison [6]
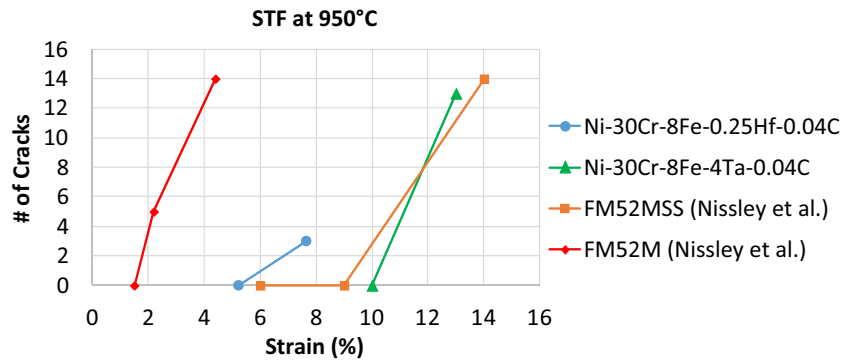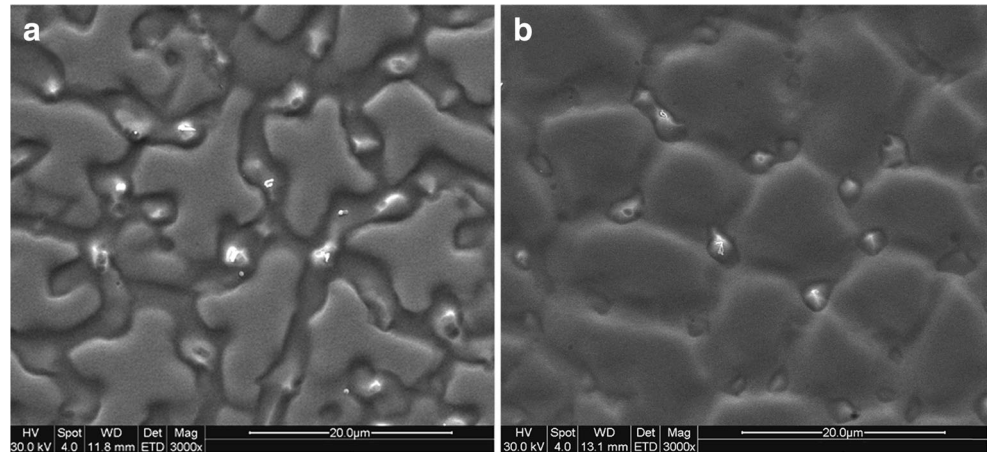

Fig. 4 SEM cross sections of Ta-bearing cast pins: **a** Alloy no. 4 with 3.86 wt% Mo and **b** alloy no. 3 without Mo addition

clear if this is related to a wetting effect. As with the Ta-bearing pins, there was no significant difference in solidification microstructure in the samples with and without Mo.

Fracture surfaces of the alloy no. 2 Hf-Mo pins were investigated due to the extremely poor resistance to solidification cracking in the CPTT test. While the cross sections show mostly discrete eutectic with a relatively low volume fraction (Fig. 5b), the eutectic apparent on the fracture surface is much different. The secondary electron image in Fig. 6a exhibits the characteristic dendritic (egg-crate) morphology indicative of solidification cracking. The backscattered image, Fig. 6b, shows a large fraction of the surface with higher Z contrast, indicating the presence of heavier elements. Qualitative EDS analysis showed these regions to be largely enriched in Hf. The area fraction of eutectic on this surface is much greater than that of the cross section, indicating that a significant amount of eutectic liquid was present at the time of fracture.

Fig. 5 SEM cross sections of Hf-bearing cast pins: **a** Alloy no. 1, without Mo addition, and **b** alloy no. 2 with 3.87 wt% Mo
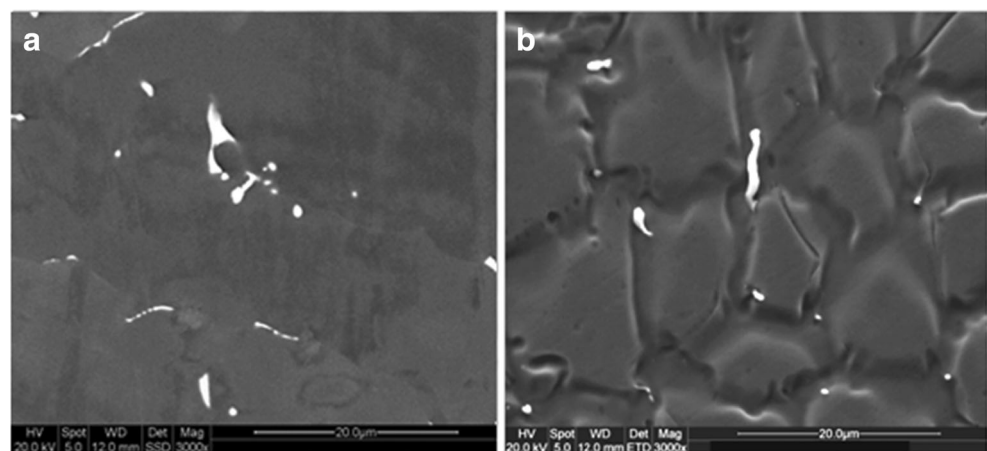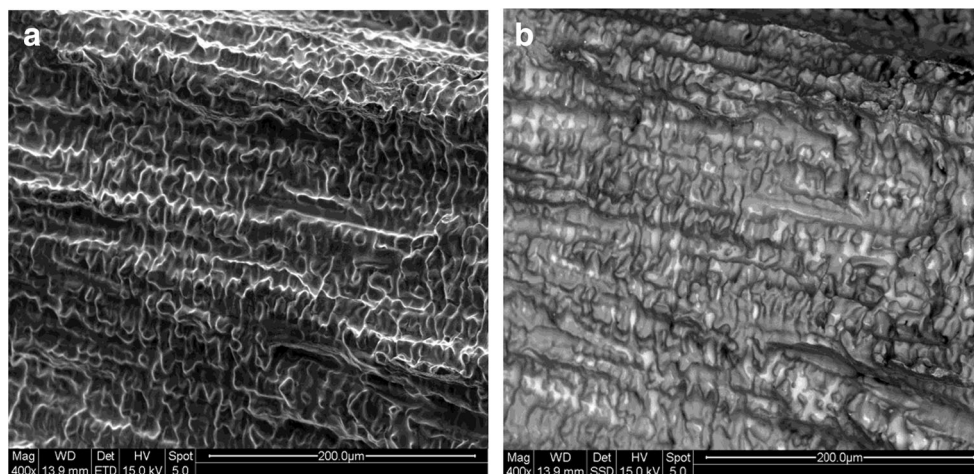
Fig. 6 Secondary electron image (a) and backscatter electron image (b) of a fracture surface in a cracked CPTT pin of Hf-Mo alloy no. 2


Grain boundaries in untested spot welds of the STF samples were characterized by light optical microscopy. Throughout the weld metal microstructure, relatively tortuous migrated grain boundaries could be found for both the Hf- and Ta-bearing weld metals. Examples of such boundaries are shown in Fig. 7. These tortuous boundaries are a result of the eutectic in both compositions pinning the crystallographic grain boundaries as they attempt to migrate away from the solidification grain boundary in the solid state. The eutectic is evenly distributed in both weld metal microstructures. Image analysis using ImageJ® determined the eutectic fraction in the Hf-bearing weld metal to be 1.2 ± 0.12 area%, while the Ta-bearing weld metal had 1.8 ± 0.15 area% eutectic fraction. These values correlate with the threshold strain to fracture, with a higher fraction eutectic leading to a higher threshold in the STF test. Both values are slightly lower than the target 2% eutectic fraction, possibly due to dilution during STF sample preparation. However, the nature of the grain boundaries is still fairly tortuous and the DDC resistance in the STF test is better than FM52M, which is known to exhibit DDC during welding.

4 Summary

The prior optimization using a DOE approach coupled with computational thermodynamic modeling led to identification of Hf- and Ta-bearing candidate alloys with potentially good resistance to weld cracking. Subsequent weldability testing revealed that the Hf-bearing alloys did not perform as expected with regard to DDC and solidification cracking susceptibility. The experimental results revealed that the optimized Hf-bearing compositions had poor solidification crack resistance in CPTT testing, which was unexpected based on the calculated, quite narrow solidification temperature range (STR). The optimized Ta- and Hf-bearing compositions showed an evenly distributed eutectic morphology that contributes to their relatively good DDC resistance in the strain to fracture (STF test). The optimized Ta-bearing composition also had good solidification cracking resistance, which has led to this alloy composition being the primary candidate for potential nuclear power industry repair and fabrication applications. Since the optimized Hf-bearing compositions had unexpectedly poor solidification crack resistance, despite a narrow STR, current research focuses on the possible influence of eutectic wetting on crack susceptibility. However, it should be

Fig. 7 Micrographs of untested STF samples of Ni-30Cr-8Fe-0.25Hf-0.04C (a) and Ni-30Cr-8Fe-4Ta-0.04C (b) showing tortuous migrated grain boundaries
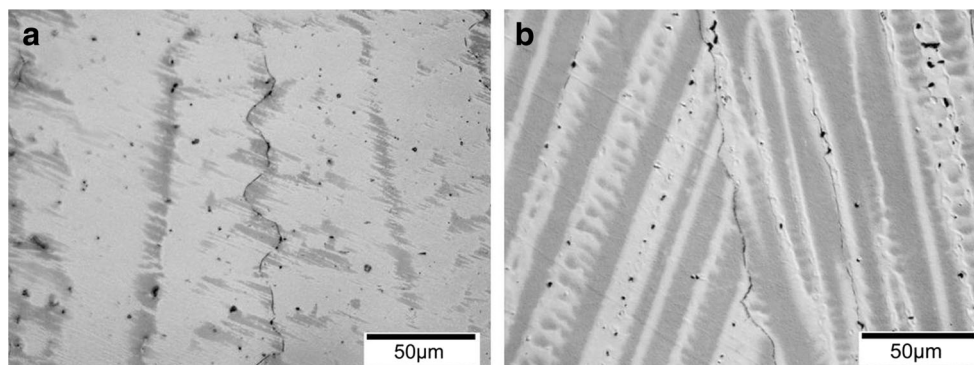
noted that CPTT and the modified STF test used to evaluate weldability in this work are particularly useful techniques for screening limited sets of alloy compositions without making actual welds, which requires the production of filler wire which can be both costly and time consuming. The methodology presented here demonstrates that a combination of computational, statistical, and experimental techniques can be extremely useful in alloy design.

References

1. Andresen PL, Morra MM (2008) Stress corrosion cracking of stainless steels and nickel alloys in high-temperature water. Corrosion 64(1):15
2. Frederick G, Lu B, King C (2008) Technical basis for preemptive weld overlays for alloy 82/182 butt welds in PWRs. (EPRI, 2008)
3. Fredette L, Scott P (2010) Evaluation of full structural and optimized weld overlays as mitigation strategies for primary water stress corrosion cracking in pressurized water reactors. (Battelle, 2010)
4. Jacko RJ, Gold RE, Kroes A (2003) Accelerated corrosion testing of alloy 52M and alloy 182 weldments. 11th Int. Conf. Environmental Degradation of Materials in Nuclear Systems
5. Kiser SD, Hinshaw EB (2005) Nickel alloy welding requirements for nuclear service. Focus on Nuclear Power Generation, pp 21–26
6. Lippold JC, Nissley NE (2008) Ductility-Dip cracking in high chromium, Ni-base filler metals. Hot Cracking Phenomena in Welds II, pp 409–425
7. Alexandrov BT et al (2011) Weldability studies of high-Cr, Ni-base filler metals for power generation applications. Weld World 55(3–4):65
8. Cieslak MJ (1991) The welding and solidification metallurgy of alloy 625. Weld J 70(2):S49–S56
9. Dupont JN, Robino CV, Marder AR (1998) Solidification and weldability of Nb-bearing superalloys. Weld J 77(10):417s–431s
10. Przybylowicz E. et al. (2016) Weldability evaluation of high chromium, Ni-base filler metals using the cast pin tear test. In: Cracking phenomena in welds IV. Springer, pp 269–288
11. Baeslack WA III (1988) Weld cracking in Ta-modified cast Inconel 718. Scr Metall 22(5):729
12. Kotval PS, Venables JD, Calder RW (1972) The role of hafnium in modifying the microstructure of cast nickel-base superalloys. Metallurgical Transactions 3(2):457
13. Dahl JM, Danesi WF, Dunn RG (1973) Partitioning of refractory metal elements in hafnium-modified cast nickel-base superalloys. Metallurgical Transactions 4(4):1087–1096
14. Dmitrieva GP, Shurin AK (1974) Investigation of phase equilibria and structure in Ni-ZrC and Ni-HfC alloys. Metallofizika 53:97–100
15. Nash P, West DRF (1981) Phase-equilibria in Ni-rich region of Ni-Cr-Hf system. Metal Science 15(8):353–356
16. Fusner E, Hope A, Lippold J 2014 Development of high-Cr, Ni-based filler metals using combined computational and experimental techniques. Weld J 93(5)
17. Nissley N (2002) Development of the strain-to-fracture test for evaluating ductility-dip cracking in austenitic stainless steels and Ni-base alloys. Welding in the World 46(7–8):32
18. Luskin T, Alexandrov BT (2012) Improvement and modeling of the cast pin tear test. AWS Professional Program, Las Vegas
19. Luskin TC (2013) Investigation of weldability in high-Cr Ni-base filler metals. The Ohio State University
20. Kreuter VC (2015) Optimization and application of the strain-to-fracture test for studying ductility-dip cracking in Ni-base alloys. The Ohio State University
21. Sowards JW (2009) Development of a chromium-free consumable for joining stainless steel. The Ohio State University
22. Feng X, Hope A, Lippold JC (2014) Effect of Cr on eutectic phase formation and solidification temperature range in Ni–Cr–Hf system. Mater Lett 116:79–81